Phytophthora infestans effector AVR3a is essential for virulence and manipulates plant immunity by stabilizing host E3 ligase CMPG1

Jorunn I. B. Bos[a], Miles R. Armstrong[b,c,1], Eleanor M. Gilroy[b,1], Petra C. Boevink[b,1], Ingo Hein[d,1], Rosalind M. Taylor[d,e], Tian Zhendong[b,f], Stefan Engelhardt[b,c], Ramesh R. Vetukuri[b,g], Brian Harrower[d], Christina Dixelius[g], Glenn Bryan[d], Ari Sadanandom[e], Stephen C. Whisson[b], Sophien Kamoun[a,2], and Paul R. J. Birch[b,c,2]

[a]The Sainsbury Laboratory, John Innes Centre, Colney, Norwich NR4 7UH, United Kingdom; [b]Plant Pathology and [d]Genetics Programmes, Scottish Crop Research Institute, Invergowrie, Dundee DD2 5DA, United Kingdom; [e]Institute of Biomedical and Life Sciences, University of Glasgow, Glasgow G12 8QQ, United Kingdom; [c]Division of Plant Sciences, College of Life Sciences, University of Dundee at the Scottish Crop Research Institute, Invergowrie, Dundee DD2 5DA, United Kingdom; [f]Department of Horticulture and Forestry Sciences, Huazhong Agricultural University, Wuhan, 430070, China; and [g]Uppsala BioCenter, Department of Plant Biology and Forest Genetics, University of Agricultural Sciences, 750 07 Uppsala, Sweden

Edited by Frederick M. Ausubel, Harvard Medical School and Massachusetts General Hospital, Boston, MA, and approved March 30, 2010 (received for review December 15, 2009)

Fungal and oomycete plant pathogens translocate effector proteins into host cells to establish infection. However, virulence targets and modes of action of their effectors are unknown. Effector AVR3a from potato blight pathogen *Phytophthora infestans* is translocated into host cells and occurs in two forms: AVR3a^{KI}, which is detected by potato resistance protein R3a, strongly suppresses infestin 1 (INF1)-triggered cell death (ICD), whereas AVR3a^{EM}, which evades recognition by R3a, weakly suppresses host ICD. Here we show that AVR3a interacts with and stabilizes host U-box E3 ligase CMPG1, which is required for ICD. In contrast, AVR3a$^{KI/Y147del}$, a mutant with a deleted C-terminal tyrosine residue that fails to suppress ICD, cannot interact with or stabilize CMPG1. CMPG1 is stabilized by the inhibitors MG132 and epoxomicin, indicating that it is degraded by the 26S proteasome. CMPG1 is degraded during ICD. However, it is stabilized by mutations in the U-box that prevent its E3 ligase activity. In stabilizing CMPG1, AVR3a thus modifies its normal activity. Remarkably, given the potential for hundreds of effector genes in the *P. infestans* genome, silencing *Avr3a* compromises *P. infestans* pathogenicity, suggesting that AVR3a is essential for virulence. Interestingly, *Avr3a* silencing can be complemented by *in planta* expression of *Avr3a^{KI}* or *Avr3a^{EM}* but not the *Avr3a$^{KI/Y147del}$* mutant. Our data provide genetic evidence that AVR3a is an essential virulence factor that targets and stabilizes the plant E3 ligase CMPG1, potentially to prevent host cell death during the biotrophic phase of infection.

oomycete | plant disease resistance | programmed cell death | ubiquitin

Two levels of inducible plant defense provide obstacles to infection. Pathogen-associated molecular pattern (PAMP)-triggered immunity (PTI) follows the perception of conserved microbial molecules at the surface of plant cells (1, 2). Plant pathogens secrete effector proteins that suppress PTI. Bacteria use a type III secretion system (T3SS) to "inject" effectors inside host cells. Characterization of the targets of bacterial T3SS effectors has revealed several biochemical mechanisms for host target modification, including manipulation of the ubiquitin proteasome system (1–4).

Effectors may be recognized by plant disease resistance (R) proteins, resulting in effector-triggered immunity (ETI) that often involves the hypersensitive response (HR), a form of programmed cell death (PCD), coinciding with restriction of the invading pathogen (1). Consequently, many pathogen effectors have evolved to suppress PCD as a component of either PTI or ETI (1, 2).

Oomycetes are eukaryotic microbes that include many devastating plant pathogens. They secrete RXLR effectors that are translocated inside host cells (5–11). The conserved motif RXLR (where R is arginine, X is any amino acid, and L is leucine) in these effectors is required for their translocation (7). RXLR effector AVR3a from *Phytophthora infestans* is represented by two alleles encoding secreted proteins that differ by only two amino acids. AVR3a^{K80I103} (AVR3a^{KI}), but not AVR3a^{E80M103} (AVR3a^{EM}) activates potato resistance protein R3a to trigger ETI (12). In addition, both forms suppress PCD induced by the *P. infestans* elicitin, infestin 1 (INF1); AVR3a^{KI} does so strongly, whereas suppression by AVR3a^{EM} is weak (13, 14). INF1 triggers a range of defense responses, including PCD in diverse plant species (15), and shares many features with PAMPs (16–18).

Recently, we showed that deletion of the C-terminal tyrosine (Y) at position 147 of AVR3a^{KI} or its replacement by the non-conservative amino acid serine (Y147S), although not affecting recognition by R3a, abolishes the ability of AVR3a^{KI} to suppress INF1-triggered cell death (ICD), allowing these two effector properties to be distinguished. In contrast, conservative replacement of Y147 by phenylalanine (Y147F) does not affect ICD suppression (14).

The aim of this research was to investigate the molecular process underlying ICD suppression by AVR3a. We show that AVR3a^{KI} strongly interacts with and stabilizes, *in planta*, the host ubiquitin E3-ligase CMPG1. CMPG1 is required for cell death mediated by INF1 (19). Stabilization and interaction are weak with AVR3a^{EM} and are lost with the AVR3a$^{KI/Y147del}$ mutant, strongly linking suppression of ICD by AVR3a with CMPG1 interaction and stabilization. Stable silencing of *Avr3a* compromises pathogenicity. This loss of virulence is readily complemented by transient expression in host cells of either *Avr3a^{KI}* or *Avr3a^{EM}* but not the *Avr3a$^{KI/Y147del}$* mutant, indicating that *Avr3a* is essential for pathogenicity and providing genetic evidence that CMPG1 is a key virulence target of *P. infestans*.

Author contributions: J.I.B.B., E.M.G., P.C.B., I.H., C.D., G.B., A.S., S.C.W., S.K., and P.R.J.B. designed research; J.I.B.B., M.R.A., E.M.G., P.C.B., I.H., R.M.T., T.Z., S.E., R.R.V., B.H., and S.C.W. performed research; J.I.B.B., M.R.A., E.M.G., P.C.B., I.H., S.C.W., S.K., and P.R.J.B. analyzed data; and J.I.B.B., M.R.A., E.M.G., P.C.B., I.H., S.K., and P.R.J.B. wrote the paper.

The authors declare no conflict of interest.

This article is a PNAS Direct Submission.

Data deposition: The sequences reported in this paper have been deposited in the GenBank database [accession nos. HM150712 (NbCMPG1-a), HM150713 (NbCMPG1-b), HM150714 (SlCMPG1), HM150715 (dN-StubCMPG1-a), and HM150716 (StubCMPG1-b)].

[1]M.R.A., E.M.G., P.C.B., and I.H. contributed equally to this work.

[2]To whom correspondence may be addressed. E-mail: pbirch@scri.ac.uk or sophien.kamoun@sainsbury-laboratory.ac.uk.

This article contains supporting information online at www.pnas.org/lookup/suppl/doi:10.1073/pnas.0914408107/-/DCSupplemental.

Results and Discussion

AVR3a Interacts with and Stabilizes Potato E3 Ubiquitin Ligase CMPG1. To investigate the molecular mechanisms underlying AVR3a-mediated cell death suppression, we identified potential host protein targets using yeast two-hybrid (Y2H) assays. We independently screened the AVR3a^{KI} and AVR3a^{EM} forms as baits against a prey library from a combination of RNA prepared at 15 h postinoculation (hpi) (early biotrophic phase), and at 72 hpi (necrotrophic phase) of a compatible (susceptible) potato interaction. Several distinct candidate AVR3a-interacting host proteins were identified (Table S1). A number of prey clones encoded a potato homolog of CMPG1 that is missing the N-terminal 29 amino acids (ΔN-StCMPG1a) (Fig. S1). CMPG1 is an ubiquitin E3 ligase that is required for cell death triggered by a range of pathogen elicitors, including INF1 (19), and thus is a potential target to explain suppression of ICD by AVR3a^{KI} (13). Consistent with AVR3a^{KI} suppressing such cell death through interaction with CMPG1, the C-terminal portion of AVR3a^{KI}, with or without RXLR–EER sequences, the AVR3a$^{KI/Y147F}$ substitution, and AVR3a^{EM} interacted with CMPG1 using Y2H, whereas no such interaction was observed with the AVR3a$^{KI/Y147S}$ or AVR3a$^{KI/Y147del}$ forms (Fig. 1*A*).

Attempts to observe *in planta* protein expression of epitope-tagged CMPG1 revealed that it was not, or was only weakly, detected using Western blot analyses and thus has low steady-state levels under the experimental conditions used. In contrast, CMPG1 was stable in yeast in the absence of AVR3a^{KI} (Fig. 1*B*). To test whether AVR3a alters the steady-state levels of CMPG1 *in planta*, *Agrobacterium tumefaciens* strains expressing 4×-myc–tagged CMPG1 from *Solanum tuberosum* (StCMPG1) were co-infiltrated with strains delivering constructs expressing FLAG-tagged AVR3a^{KI}, AVR3a^{EM}, AVR3a$^{KI/Y147del}$, or a vector control in *Nicotiana benthamiana*. Western blot analysis of leaf tissues harvested at 2, 3, and 5 d postinfiltration (dpi) showed that the ΔN-StCMPG1a protein was stabilized in the presence of AVR3a^{KI} at 3 dpi (Fig. 1*C*). By 5 dpi, both AVR3a^{KI} and AVR3a^{EM}, but not AVR3a$^{KI/Y147del}$, stabilized CMPG1 equally well compared with the vector control (Fig. 1*D*). This finding suggests that AVR3a^{KI} has stronger CMPG1 stabilization activity than AVR3a^{EM}, consistent with its stronger ICD suppression activity. The failure of AVR3a$^{KI/Y147del}$ to stabilize CMPG1 is consistent with its loss of ICD suppression. Interestingly, AVR3a-stabilized CMPG1 was detected as a double band by Western analyses, suggesting that CMPG1 may be modified.

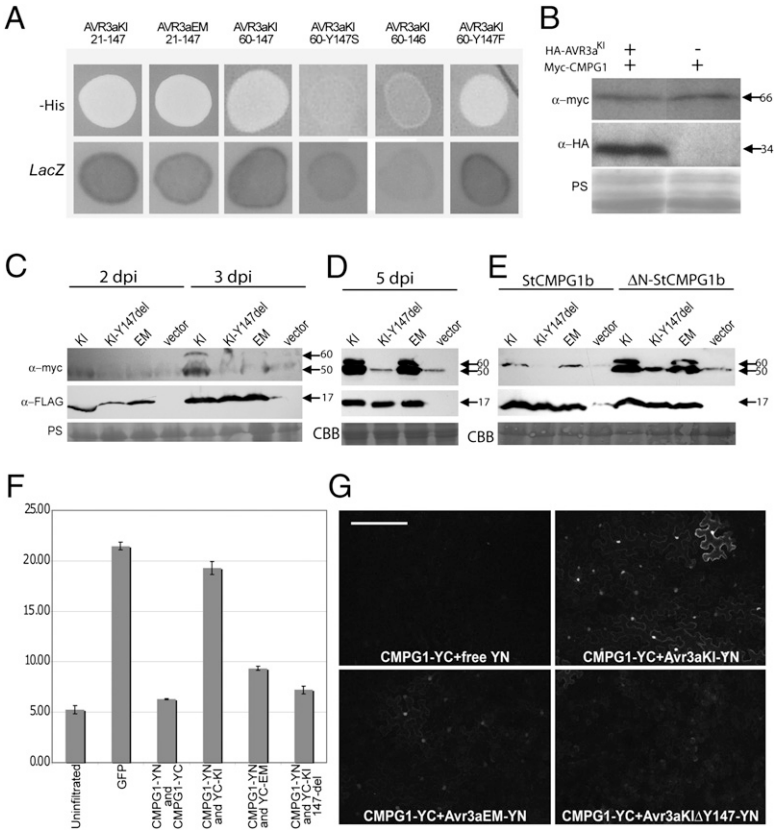

Fig. 1. AVR3a^{KI} and AVR3a^{EM} interact with and stabilize CMPG1. (*A*) AVR3a^{KI} and AVR3a^{EM} with (21-147) and without (60-147; shown only for AVR3a^{KI}) RXLR-encoding portions interact with CMPG1 in Y2H (LacZ and -His reporter genes activated). Whereas AVR3a$^{KI/Y147del}$ (Y147 deletion) and AVR3a$^{KI/Y147S}$ mutants fail to interact with CMPG1, the AVR3a$^{KI/Y147F}$ mutant interacts. (*B*) Western blots probed with anti-myc and anti-HA antibodies following expression of mycCMPG1 in binding domain vector, with or without HA-AVR3a^{KI} in activation domain vector, in yeast. (*C*) Western blots probed with anti-myc and anti-FLAG antibodies, showing a time course of transient coexpression (by agroinfiltration) of FLAG-AVR3a^{KI}, FLAG-AVR3a^{EM}, FLAG- AVR3a$^{KI/Y147del}$, or a vector control with 4×-myc-ΔN-StCMPG1a at 2 and 3 dpi. (*D*) As in *C*, but at 5 dpi. (*E*) As in *C* but at 5 dpi with 4×-myc-StCMPG1b (full-length) and 4×-myc-ΔN-StCMPG1b (lacking the N-terminal 29 amino acids). Protein sizes are indicated in kDa. Protein loading is shown by Coomassie blue (CBB) or Ponceau S (PS) staining. (*F*) Fluorimeter measurements (in relative fluorescence units) following coexpression in *N. benthamiana* of the split YFP constructs CMPG1::N-YFP (YN), CMPG1::C-YFP (YC), C-YFP::AVR3a^{KI}, C-YFP::AVR3a^{EM}, and C-YFP::AVR3a$^{KI/Y147del}$, as indicated. (*G*) Confocal microscopy following coexpression in *N. benthamiana* of split YFP constructs CMPG1-YC with a vector expressing free N-YFP and CMPG1-YC with N-YFP::AVR3a^{KI}, N-YFP::AVR3a^{EM}, and N-YFP::AVR3a$^{KI/Y147del}$ constructs as indicated in the panels. (Scale bars, 200 μm.)

At 5 dpi, AVR3a^{KI} and AVR3a^{EM}, but not the AVR3a$^{KI/Y147del}$ mutant, also stabilizedStCMPG1b (Fig. 1*E*), a full-length CMPG1 protein from *S. tuberosum* that differs by 11 amino acids from StCMPG1a (Fig. S1). However, stabilization of full-length StCMPG1b was reduced compared with a truncated version, ΔN-StCMPG1b, which is missing the 29 N-terminal amino acids (Fig. 1*E*). In addition, full-length proteins encoded by two different *CMPG1* genes from *N. benthamiana* (Nb) and one from *S. lycopersicum* (Sl) (Fig. S1), two plants that are hosts for *P. infestans,* also were stabilized at 5 dpi by AVR3a^{KI} and AVR3a^{EM} but not by AVR3a$^{KI/Y147del}$ upon coexpression in *N. benthamiana* (Fig. S2*A*).

To verify independently that AVR3a^{KI} more strongly stabilizes CMPG1, *CFP-Avr3a^{KI}*, *CFP-Avr3a^{EM}*, and *CFP- Avr3a$^{KI/Y147del}$* constructs (generating N-terminal fusions to CFP) were each coexpressed with *StCMPG1b-YFP* (expressing full-length StCMPG1b fused to YFP) and visualized at 2 and 3 dpi using confocal microscopy. Whereas CFP fluorescence was similar in each experiment, indicating similar levels of CFP-AVR3a^{KI}, CFP-AVR3a^{EM}, and CFP-AVR3a$^{KI/Y147del}$ proteins, CMPG1-YFP fluorescence was significantly stronger following coexpression with CFP-AVR3a^{KI} than with CFP::AVR3a^{EM} and was barely detectable with CFP-AVR3a$^{KI/Y147del}$, again indicating that AVR3a^{KI} more strongly stabilizes CMPG1 (Fig. S2 *B–D*).

Further analysis *in planta* of the interaction was performed with bimolecular fluorescence complementation. N- or C-terminus–encoding portions of *YFP* were fused to *Avr3a^{KI}, Avr3a^{EM}, Avr3a$^{KI/Y147del}$*, or full-length *StCMPG1b,* and constructs containing complementary halves of YFP were coexpressed in *N. benthamiana*. Whereas combinations of *StCMPG1-N/C-YFP* with corresponding *N/C-YFP-Avr3a^{KI}* fusions yielded strong fluorescence, measured using a fluorimeter (Fig. 1*F*) and assessed using confocal microscopy (Fig. 1*G*), fluorescence was weak following coexpression of *StCMPG1-N/C-YFP* fusions with *N/C-YFP-Avr3a^{EM}* fusions and was barely detectable with *N/C-YFP- Avr3a$^{KI/Y147del}$* fusions (Fig. 1 *F* and *G*). To investigate whether these differences were caused by stabilization of CMPG1 by the nonmutant forms of AVR3a, *StCMPG1-N/C-YFP* fusions also were coexpressed with either *N/C-YFP-Avr3a^{KI}* or *N/C-YFP- Avr3a$^{KI/Y147del}$* fusions in the presence of untagged *AVR3a^{KI}* (to stabilize CMPG1). Again strong fluorescence was seen only with coexpression of *StCMPG1-N/C-YFP* and *N/C-YFP-Avr3a^{KI}* fusions (Fig. S2*E*). These results support the lack of interaction between AVR3a$^{KI/Y147del}$ and CMPG1 seen in Y2H and suggest that the interaction *in planta* between AVR3a^{KI} and CMPG1 is stronger than that observed between AVR3a^{EM} and CMPG1.

The inability of the AVR3a$^{KI/Y147del}$ mutant to interact with and stabilize CMPG1 is consistent with previous observations that this mutant is unable to suppress ICD (14). Moreover, the weak stabilization of CMPG1 by AVR3a^{EM} corresponds to weak inhibition of INF1-triggered PCD, further supporting the deduction that AVR3a suppresses ICD through its action on CMPG1. Although the AVR3a$^{KI/Y147del}$ mutant fails to interact with or stabilize CMPG1, it nevertheless triggers R3a-mediated HR (Figs. S2 and S3) (14), indicating that CMPG1 is not involved in this defense response. Indeed, silencing of *NtCMPG1* by RNAi did not compromise R3a-triggered HR (Fig. S3), demonstrating that CMPG1 is not a "guardee" mediating recognition of AVR3a^{KI} by R3a (20). Taken together, our data indicate that CMPG1 is a host target of AVR3a and is stabilized by it *in planta.*

Stabilization of CMPG1 Also Occurs Following Its Inactivation. If suppression of ICD by AVR3a is caused by stabilization of CMPG1, we hypothesized that, during ICD, CMPG1 steady-state levels should not increase in the absence of AVR3a. As expected, coexpression of 4×-myc-ΔN-StCMPG1a with INF1 did not stabilize CMPG1 compared with the vector control at the onset of cell death symptoms (3 dpi), whereas AVR3a^{KI} did (Fig. 2*A*). This finding was confirmed by coexpression of *INF1* with *StCMPG1b-YFP*, in which no YFP fluorescence was detected throughout a time course of 1–3 dpi, before INF1-triggered cell death. Thus, CMPG1-mediated cell death does not require CMPG1 stabilization.

An explanation for the low abundance of CMPG1 in the absence of AVR3a is that it is degraded by the 26S proteasome. We therefore tested whether the 26S proteasome inhibitors MG132 and epoxomicin could stabilize CMPG1. We expressed 4×-myc-ΔN-StCMPG1a in the presence of MG132, epoxomicin, or buffer control. In the absence of AVR3a^{KI}, we observed an increase in CMPG1 protein levels after MG132 (Fig. 2*B*) and epoxomicin (Fig. 2 *C–E*) treatments, indicating that degradation of CMPG1 is dependent on the 26S proteasome. The epoxomicin treatment resulted in stronger stabilization of CMPG1 and a double band reminiscent of stabilization in the presence of AVR3a^{KI} (Fig. 2*C*).

Because CMPG1 is constantly degraded by the 26S proteasome, we tested whether mutations C37A and W64A in full-length NbCMPG1a, previously shown to abolish E3 ligase activity in vitro and to act as dominant negatives to prevent ICD (19), affected CMPG1 stability. As expected, coexpression of NbCMPG1a (Fig. S1) with AVR3a^{KI} in *N. benthamiana* resulted in stabilization compared with the vector control (Fig. 2*F*). In the absence of AVR3a, NbCMPG1aC37A and NbCMPG1aW64A proteins were detectable at higher levels than the wild-type protein, suggesting that the mutations in the U-box domain stabilized CMPG1. However, in the presence of AVR3a these inactive forms of CMPG1 were more strongly stabilized and modified, as indicated by the upper band in Western assays (Fig. 2*F*). Stabilization of CMPG1 following inactivation of the U-box suggests that its E3 ligase activity contributes to its instability, possibly through self-ubiquitination and degradation. The further stabili-

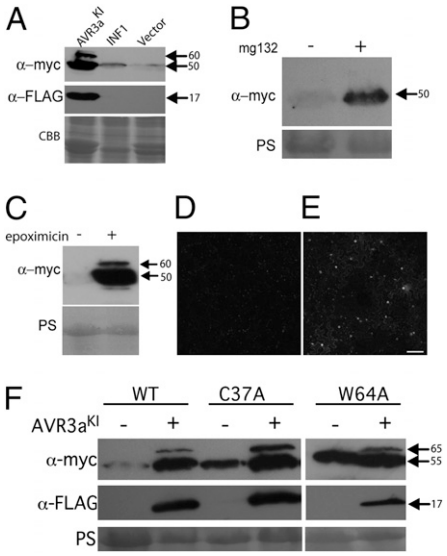

Fig. 2. CMPG1 stabilization is consistent with its inactivation or modification. (*A*) Western blot probed with anti-myc and anti-FLAG antibodies following coexpression of 4×-myc-ΔN-StCMPG1a with FLAG-AVR3a^{KI}, with INF1, or with empty vector control. (*B*) Western blots probed with anti-myc antibody, following expression of ΔN-4×-myc-StCMPG1a with or without MG132 inhibitor treatment as indicated. (*C*) Western blot probed as in *B* following expression of ΔN-4×-myc-StCMPG1a with or without epoxomicin inhibitor treatment. Confocal images of CMPG1-YFP following water (*D*) or epoxomicin (*E*) treatment. (Scale bar, 200 μm.) (*F*) Western blot probed as in *A* following expression of 4×-myc-NbCMPG1a, 4×-myc-NbCMPG1aC34A, or 4×-myc-NbCMPG1aW64A with or without FLAG-AVR3a^{KI}. Sizes are indicated in kDa. Protein loading is shown by Coomassie blue (CBB) or Ponceau S (PS) staining.

zation and modification by AVR3a may be explained by its action on endogenous, wild-type CMPG1 in this transient expression assay.

With AVR3a, as with epoxomicin, we see accumulation of a modified form of CMPG1. Critically, to prevent ICD, these experiments indicate that stabilization of CMPG1 by AVR3a is consistent with modification of its activity to prevent the normal degradation of itself, and thus, potentially, its substrates in the host cell.

CMPG1 Activity Is Important for *P. Infestans* Pathogenicity. To determine the role of CMPG1 during *P. infestans* infection, we first confirmed the biological significance of CMPG1 stabilization by AVR3a. We detected CMPG1 stabilization in *P. infestans*-infected *N. benthamiana* leaves that were transiently expressing 4×-myc-ΔN-StCMPG1a (Fig. 3 *A* and *B*). Stabilization was detected with isolate 88069 ($AVR3a^{EM}$ homozygote) and isolate CA65 ($AVR3a^{KI}$ homozygote). Although $AVR3a^{EM}$ exhibits weaker ICD suppression activity than $AVR3a^{KI}$ in transient overexpression assays, it is possible that in a natural infection this activity is sufficient for AVR3a virulence function.

At the onset of infection we observed that *NbCMPG1* transcripts accumulated rapidly following inoculation of *P. infestans* onto leaves (Fig. S4). This observation is consistent with previous reports of rapid *CMPG1* up-regulation (19, 21) and suggests that CMPG1 may contribute to PTI. *Avr3a* is transcriptionally up-regulated in germinating cysts and during the first 1–3 dpi (12) (Fig. S4), indicating that its synthesis coincides with early up-regulation of *CMPG1*. As observed previously (22, 23), *INF1* transcript decreased during the biotrophic phase (Fig. S4). This decrease indicates that, in addition to early targeting of CMPG1 by AVR3a, *P. infestans* subsequently reduces its potential to elicit CMPG1-mediated PCD during biotrophy, an activity that is consistent with evasion of PTI. In support of this notion, it has been shown previously that an isolate of *P. infestans* that is silenced for *INF1* expression more readily establishes infection of *N. benthamiana* (24).

A number of lines of evidence indicate that CMPG1 activity may contribute to the necrotrophic phase of *P. infestans* infection. During this phase, transcript accumulation of *Avr3a* decreases markedly, potentially reducing the pathogen's capacity to stabilize CMPG1 (Fig. S4) (7). Conversely, at the onset of necrotrophy, both *INF1* and *CMPG1* transcripts were seen to accumulate coordinately, suggesting that necrotrophy may involve host PCD that is stimulated by the pathogen (Fig. S4). Consistent with this suggestion, the host cysteine protease cathepsin B, which is involved in PCD (25, 26), is induced at a similar stage (3 dpi) of a compatible interaction between potato and *P. infestans* (27).

To investigate further the role of CMPG1 in the necrotrophic phase, we silenced *CMPG1* in *N. benthamiana* and challenged silenced leaves with *P. infestans*. In TRV::*GFP* plants infection extended across the leaf, with massive sporulation by 6 dpi (Fig. 3*C*). In contrast, infection of plants inoculated with TRV::*NbCMPG1* showed significantly reduced sporulation (Fig. 3 *C* and *E* and Fig. S5) and lesion diameter (Fig. 3 C and *F*), indicating that NbCMPG1 activity positively impacts the late stages of *P. infestans* infection. *NbCMPG1* transcript levels were reduced in TRV::*NbCMPG1* plants to 25% of the levels in control TRV::*GFP* plants (Fig. 3*D*).

Stabilization of CMPG1 during infection indicates that it is a target for suppression of PTI. Nevertheless, remarkably, CMPG1 activity is required for *P. infestans* during the late, necrotrophic phase of infection. A reasonable explanation is that host defenses that are suppressed by a hemibiotrophic pathogen at early stages of colonization may be actively provoked to the pathogen's benefit at later stages. Although these results were unexpected, Arabidopsis RIN4, a widely studied target of bacterial effectors, is known to have contrasting functions, because this protein both positively and negatively regulates plant immunity (28).

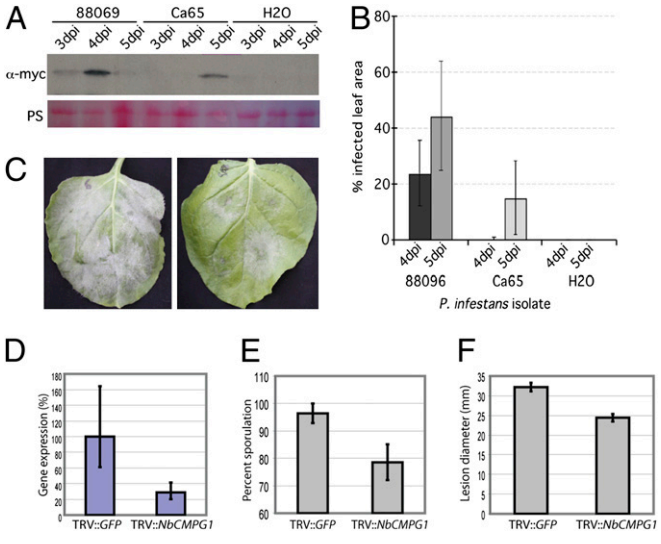

Fig. 3. CMPG1 is stabilized during infection. (*A*) Western blot probed with anti-myc antibody indicating stabilization of constitutively expressed ΔN-StCMPG1a-4×-myc across a time course of *N. benthamiana* infection with *P. infestans* isolates 88069 and CA65. (*B*) Disease development, measured as per cent infected leaf area, of isolates 88069 and CA65 on *N. benthamiana* at 4 and 5 dpi. (*C*) Typical infection of *P. infestans* isolate 88069 on TRV::*GFP*-inoculated *N. benthamiana* (*Left*) and TRV::*CMPG1*-inoculated *N. benthamiana* (*Right*) at 6 dpi. (*D*) Real-time RT-PCR showing relative expression of *NbCMPG1* in *N. benthamiana* plants inoculated with TRV::*GFP* and TRV::*CMPG1*. (*E*) Percentage of *P. infestans* infection lesions that developed sporangia on TRV::*GFP* and TRV::*CMPG1*-inoculated *N. benthamiana* leaves at 6 dpi. (*F*) Diameter (mm) of *P. infestans* infection lesion in TRV::*GFP* and TRV::*CMPG1*-inoculated *N. benthamiana* leaves at 6 dpi. Vector-induced gene-silencing experiments were repeated on six occasions with six replicate plants for each construct, with reproducible results.

***Avr3a* Is Essential for Virulence.** To investigate the contribution of AVR3a to virulence, isolate 88069 was transformed with constructs designed to silence *Avr3a* stably. A silenced line (CS12) was selected with *Avr3a* expression less than 5% of wild-type levels. The silenced line grew and sporulated normally in vitro but was significantly reduced in pathogenicity on susceptible *Solanum tuberosum* cv Bintje (Fig. 4*A*), and on *N. benthamiana* (Fig. 4 *B* and *C*).

We hypothesized that transient expression of *Avr3a* inside plant cells could complement the loss of virulence of CS12. Transient expression of $CFP\text{-}Avr3a^{KI}$ in *N. benthamiana* led to detectable CFP fluorescence up to 5 d after agroinfiltration (dpi), indicating that its expression was silenced by this time (Fig. S6). We thus surmised that if *P. infestans* were inoculated on the plants at 2 dpi, transient expression of *Avr3a* constructs in plant cells would persist only for the biotrophic phase of infection. Strikingly, transient expression of either $Avr3a^{EM}$ (Fig. 4 *D* and *E*) or $Avr3a^{KI}$ in plant cells (Fig. 4 *F* and *G*) restored virulence levels of CS12 to those of wild-type 88069 (Fig. 4*H*). In contrast, we observed no complementation of the *Avr3a*-silenced phenotype following transient expression of $Avr3a^{KI/Y147del}$ (Fig. S7).

These results indicate that *Avr3a* is essential for virulence during the biotrophic phase. Moreover, they indicate that deletion of the terminal tyrosine from $AVR3a^{KI}$, although not affecting recognition by R3a, prevents either suppression of ICD or restoration of virulence to the *AVR3a*-silenced CS12 line.

Although little is known about the functions of eukaryote plant pathogen effectors, bacterial plant pathogen T3SS effectors sup-

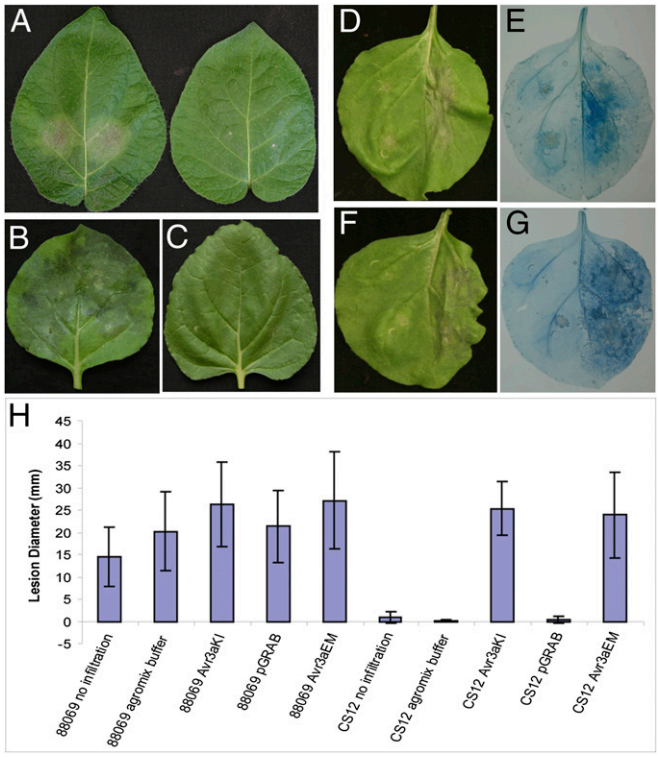

Fig. 4. *Avr3a* is essential for virulence. (*A*) Infection of potato cultivar Bintje by wild-type *P. infestans* isolate 88069 (left leaf) and *Avr3a*-silenced line CS12 (right leaf) at 4 dpi. (*B*) Infection of *N. benthamiana* by wild-type *P. infestans* isolate 88069 at 6 dpi. (*C*) Infection of *N. benthamiana* by *Avr3a*-silenced line CS12 at 6 dpi. (*D*) Infection of *N. benthamiana* by *Avr3a*-silenced line CS12 at 6 dpi, following agroexpression of pGRAB::$Avr3a^{EM}$ (left half of leaf) or empty pGRAB (right half of leaf). (*E*) As in *D*, but leaf is stained with trypan blue. (*F*) Infection of *N. benthamiana* by *Avr3a*-silenced line CS12 at 6 dpi, following agroexpression of pGRAB::$Avr3a^{KI}$ (left half of leaf) or empty pGRAB (right half of leaf). (*G*) As in *F*, but leaf is stained with trypan blue. (*H*) Measurements at 6 dpi of lesion sizes (mm) following infection of isolate 88069 or silenced line CS12 on leaves that were uninfiltrated, infiltrated with agromix, agroinfiltrated to express $AVR4a^{KI}$, $Avr3a^{EM}$, or empty pGRAB vector. These complementation experiments were repeated on four occasions, with leaves from six plants for each treatment/construct.

press PTI and ETI by a number of enzymatic activities, through direct protein–protein interactions with defense-associated host targets (1–4). The *Pseudomonas syringae* T3SS effector AvrPtoB exhibits ubiquitin E3 ligase activity which is required to suppress plant innate immunity, indicating that bacterial plant pathogens can modulate the host ubiquitin proteasome system (29, 30). Oomycete plant pathogens also translocate RXLR effector proteins into host cells to promote susceptibility (7, 9, 10). We show that *P. infestans* RXLR effector AVR3a, which suppresses PCD triggered by the PAMP-like elicitin INF1 (ICD) (13, 14), interacts with and stabilizes the host ubiquitin E3 ligase CMPG1, which is required for ICD (19). An $Avr3a^{KI/Y147del}$ mutant that lacks cell death suppression activity did not interact with or stabilize CMPG1. Stabilization of CMPG1 by AVR3a thus is consistent with the ability of this effector to suppress ICD by modifying CMPG1 activity, preventing the normal 26S proteasome-dependent degradation of itself and thus potentially of its protein substrates in the host cell. In addition, we show that AVR3a, unlike many bacterial T3SS effectors, and despite the presence of hundreds of candidate RXLR effector genes in the *P. infestans* genome (31), is essential for virulence and thus is functionally non-redundant. Critically, because the $Avr3a^{KI/Y147del}$ mutant cannot suppress ICD or interact with or stabilize CMPG1, its failure to complement the *AVR3a*-silenced *P. infestans* line strongly implicates these activities in AVR3a's essential contribution to virulence. We report a plant host target of a translocated effector from a filamentous eukaryotic plant pathogen and show that this effector, like some bacterial effectors (32), is able to manipulate the host ubiquitin proteasome system to suppress plant immunity.

Materials and Methods

Microbial Strains and Growth Conditions. *A. tumefaciens* strain GV3101 was used in molecular cloning experiments and was routinely cultured at 28 °C in LB medium using appropriate antibiotics (32). *P. infestans* isolates Ca65 and 88069 and silenced line CS12 were maintained on rye sucrose agar plates as previously described (7).

Plasmid Constructs. The constructs pGR106-FLAG-$AVR3a^{KI}$ and FLAG-$AVR3a^{EM}$ Δ23–147 were described previously (13), as was pGR106-$AVR3a^{KI/Y147del}$ mutant (Δ23–146) with an N-terminal FLAG tag (14). All additional *Avr3a* constructs for Y2H, for agroexpression *in planta* and for fluorescent protein fusion and all *CMPG1* constructs for equivalent experiments were cloned using the GATEWAY cloning system (Invitrogen); details are given in *SI Text* and Table S2.

Y2H Screens. Y2H screening was performed using the ProQuest system (Invitrogen). Details are given in *SI Text*.

Agroinfiltration Assays to Investigate CMPG1 Stabilization by Western Analyses. Recombinant *A. tumefaciens* strains were grown as described previously (33), except that the culturing steps were performed in LB medium supplemented with 50 μg/mL of kanamycin. Agroinfiltration experiments were performed on 4- to 6-week-old *N. benthamiana* or *N. tabacum* plants as appropriate. Plants were grown and maintained throughout the experiments in a greenhouse with an ambient temperature of 22–25 °C and high light intensity. Precise details of each agro-expression assay are provided in *SI Text*.

INF1 Protein Infiltration. INF1 protein was produced in *Escherichia coli* carrying a pFLAG-ATS-INF1 expression construct as previously described (24). Supernatants were infiltrated in RNAi stable transgenic tobacco and wild-type tobacco in different dilutions (2×, 5×, 10×, and 15×).

Western Blot Analyses. Samples for SDS/PAGE were prepared by grinding leaf tissue in liquid nitrogen followed by boiling for 5 min in SDS-loading buffer supplemented with 50 uM DTT. The presence of recombinant myc-CMPG1 and FLAG-AVR3a *in planta* was determined by SDS/PAGE and Western blotting as described by Tian et al. (34). For detection of CMPG1, Western blots were incubated overnight with myc-antibodies diluted 1:4,000 in PBS-T with 5% milk. Incubation with a secondary anti-rabbit HRP-conjugated antibody was performed for 1 h. Protein bands on Western blots were detected using ECL substrate (Thermo Scientific Pierce). Additional Western blot methods are described in *SI Text*.

Confocal Imaging. *N. benthamiana* plants were grown in a greenhouse at 22 °C (day temperature) and 18 °C (night temperature) with a minimum of 16 h light. *A. tumefaciens* transient expression was performed as described in *SI Text*. Imaging was conducted on a Leica TCS-SP2 AOBS (Leica Microsystems) using HCX APO L 20×/0.5, 40×/0.8 and 63×/0.9 water-dipping lenses as described in detail in *SI Text*. PhotoshopCS software (Adobe Systems) was used for postacquisition image processing. Quantification of fluorescence was performed using a SpectraMax M5 fluorimeter (Molecular Devices) as described in *SI Text*.

Quantitative RT-PCRs. *N. benthamiana* leaves from 20 plants were sprayed with a *P. infestans* sporangia suspension of isolate 88069. Five leaves were collected each day through a time course from 0 to 5 d. Sporangia cDNA from 88069 was prepared as described in (7). Total RNA was extracted from the pooled leaf sample using RNeasy Minikit (Qiagen). cDNA was synthesized from 3 μg of total RNA using random primers (Applied Biosystems) with SuperScript II Reverse Transcriptase (Invitrogen) according to manufacturers" instructions. cDNA was diluted by a factor of 10, and 2 μL was used per well with Power SYBR Green PCR Master Mix (Applied Biosystems) in 25-μL reactions. Each PCR was performed in duplicate on a Chromo4 RT-PCR detector with DNA Engine Peltier Thermal Cycler (Bio-Rad) as described in *SI Text*.

Transformation of *P. Infestans*, Silencing of *Avr3a*^{EM}, and Testing Silencing Phenotype. The *PiAvr3a* gene was cloned as an inverted repeat, with the inverted copies separated by a 1,422-bp intron (from AY310901) from the *Petunia hybrida* chalcone synthase (CS) gene as described in *SI Text*. Stable transformation of *P. infestans* isolate 88069 (homozygous *Avr3a*^{EM}) was achieved using a modified polyethylene glycol (PEG)–$CaCl_2$–Lipofectin protocol (*SI Text*). Modifications to this protocol were as described in Grouffaud et al. (35). Sporangia were harvested from cultures of silenced transformant CS12 and wild-type 88069 by flooding with sterile water, gentle rubbing with a glass rod, decanting of the solution, and centrifugation at 700 × *g* for 5 min. Inoculation of detached *S. tuberosum* cv. Bintje leaves and leaves of whole *N. benthamiana* plants was performed as described in Whisson et al. (7). Complementation in *N. benthamiana* is described in detail in *SI Text*.

Virus-Induced Gene Silencing of *NbCMPG1*. Viral-induced gene silencing was performed using binary Tobacco Rattle Virus (TRV) vectors in *N. benthamiana*. For *NbCMPG1* silencing, a 250-bp fragment from within the equivalent region used for the *NtCMPG1* RNAi hairpin (6) was cloned in antisense as described in *SI Text*. A TRV construct expressing GFP was used as a control as described in Gilroy et al. (25). Analysis of virus-induced gene silencing in plants 3–4weeks postinoculation with viruses by qRT-PCR and *P. infestans* inoculations on viral-induced gene-silenced plants are described in *SI Text*.

ACKNOWLEDGMENTS. We thank J. Jones (The Sainsbury Laboratory, Norwich, UK) for providing the CMPG1 RNAi tobacco lines, I. Malcuit (The Sainsbury Laboratory, Norwich, UK) and D. Baulcombe (University of Cambridge, Cambridge, UK) for providing the PVX vector, J. Lindbo for the pJL3-p19 vector, H. S. Judelson for helpful suggestions to determine expression of sporulation-associated genes from *P. infestans*, and S. Schornack and E. Huitema for suggestions and comments on the manuscript. This work was supported by the Gatsby Charitable Foundation at The Sainsbury Laboratory and by the Rural and Environment Research and Analysis Directorate and Biotechnology and Biological Sciences Research Council funding at the Universities of Dundee and Glasgow and at the Scottish Crop Research Institute.

1. Jones JD, Dangl JL (2006) The plant immune system. *Nature* 444:323–329.
2. Chisholm ST, Coaker G, Day B, Staskawicz BJ (2006) Host-microbe interactions: Shaping the evolution of the plant immune response. *Cell* 124:803–814.
3. Block A, Li G, Fu ZQ, Alfano JR (2008) Phytopathogen type III effector weaponry and their plant targets. *Curr Opin Plant Biol* 11:396–403.
4. Grant SR, Fisher EJ, Chang JH, Mole BM, Dangl JL (2006) Subterfuge and manipulation: Type III effector proteins of phytopathogenic bacteria. *Annu Rev Microbiol* 60:425–449.
5. Kamoun S (2006) A catalogue of the effector secretome of plant pathogenic oomycetes. *Annu Rev Phytopathol* 44:41–60.
6. Kamoun S (2007) Groovy times: Filamentous pathogen effectors revealed. *Curr Opin Plant Biol* 10:358–365.
7. Whisson SC, et al. (2007) A translocation signal for delivery of oomycete effector proteins into host plant cells. *Nature* 450:115–118.
8. Birch PRJ, Rehmany AP, Pritchard L, Kamoun S, Beynon JL (2006) Trafficking arms: Oomycete effectors enter host plant cells. *Trends Microbiol* 14:8–11.
9. Dou D, et al. (2008) RXLR-mediated entry of *Phytophthora sojae* effector *Avr1b* into soybean cells does not require pathogen-encoded machinery. *Plant Cell* 20:1930–1947.
10. Birch PRJ, et al. (2008) Oomycete RXLR effectors: Delivery, functional redundancy and durable disease resistance. *Curr Opin Plant Biol* 11:373–379.
11. Hein I, Gilroy EM, Armstrong MR, Birch PRJ (2009) The zig-zag-zig in oomycete-plant interactions. *Mol Plant Pathol* 10:547–562.
12. Armstrong MR, et al. (2005) An ancestral oomycete locus contains late blight avirulence gene Avr3a, encoding a protein that is recognized in the host cytoplasm. *Proc Natl Acad Sci USA* 102:7766–7771.
13. Bos JIB, et al. (2006) The C-terminal half of *Phytophthora infestans* RXLR effector AVR3a is sufficient to trigger R3a-mediated hypersensitivity and suppress INF1-induced cell death in *Nicotiana benthamiana*. *Plant J* 48:165–176.
14. Bos JIB, Chaparro-Garcia A, Quesada-Ocampo LM, McSpadden Gardener BB, Kamoun S (2009) Distinct amino acids of the *Phytophthora infestans* effector AVR3a condition activation of R3a hypersensitivity and suppression of cell death. *Mol Plant Microbe Interact* 22:269–281.
15. Vleeshouwers VGAA, et al. (2006) Agroinfection-based high-throughput screening reveals specific recognition of INF elicitins in *Solanum*. *Mol Plant Pathol* 7:499–510.
16. Hann DR, Rathjen JP (2007) Early events in the pathogenicity of *Pseudomonas syringae* on *Nicotiana benthamiana*. *Plant J* 49:607–618.
17. Kawamura Y, et al. (2009) INF1 elicitin activates jasmonic acid- and ethylene-mediated signalling pathways and induces resistance to bacterial wilt disease in tomato. *J Phytopathol* 157:287–297.
18. Heese A, et al. (2007) The receptor-like kinase SERK3/BAK1 is a central regulator of innate immunity in plants. *Proc Natl Acad Sci USA* 104:12217–12222.
19. González-Lamothe R, et al. (2006) The U-box protein CMPG1 is required for efficient activation of defense mechanisms triggered by multiple resistance genes in tobacco and tomato. *Plant Cell* 18:1067–1083.
20. van der Hoorn RAL, Kamoun S (2008) From guard to decoy: A new model for perception of plant pathogen effectors. *Plant Cell* 20:2009–2017.
21. Heise A, Lippok B, Kirsch C, Hahlbrock K (2002) Two immediate-early pathogen-responsive members of the AtCMPG gene family in *Arabidopsis thaliana* and the W-box-containing elicitor-response element of AtCMPG1. *Proc Natl Acad Sci USA* 99:9049–9054.
22. Haas B, et al. (2009) The genome sequence of the Irish famine pathogen *Phytophthora infestans*. *Nature* 461:393–398.
23. Kamoun S, et al. (1997) A gene encoding a protein elicitor of *Phytophthora infestans* is down-regulated during infection of potato. *Mol Plant Microbe Interact* 10:13–20.
24. Kamoun S, et al. (1998) Resistance of *Nicotiana benthamiana* to *Phytophthora infestans* is mediated by the recognition of the elicitor protein INF1. *Plant Cell* 10:1413–1426.
25. Gilroy EM, et al. (2007) Involvement of cathepsin B in the plant disease resistance hypersensitive response. *Plant J* 52:1–13.
26. McLellan H, Gilroy EM, Yun B-W, Birch PRJ, Loake GJ (2009) Functional redundancy in the *Arabidopsis Cathepsin B* gene family contributes to basal defence, the hypersensitive response and senescence. *New Phytol* 183:408–418.
27. Avrova AO, et al. (2004) Potato oxysterol binding protein and cathepsin B are rapidly up-regulated in independent defence pathways that distinguish *R* gene-mediated and field resistances to *Phytophthora infestans*. *Mol Plant Pathol* 5:45–56.
28. Mackey D, Belkhadir Y, Alonso JM, Ecker JR, Dangl JL (2003) Arabidopsis RIN4 is a target of the type III virulence effector AvrRpt2 and modulates RPS2-mediated resistance. *Cell* 112:379–389.
29. Abramovitch RB, Janjusevic R, Stebbins CE, Martin GB (2006) Type III effector AvrPtoB requires intrinsic E3 ubiquitin ligase activity to suppress plant cell death and immunity. *Proc Natl Acad Sci USA* 103:2851–2856.
30. Rosebrock TR, et al. (2007) A bacterial E3 ubiquitin ligase targets a host protein kinase to disrupt plant immunity. *Nature* 448:370–374.
31. Haas BJ, et al. (2009) Genome sequence and analysis of the Irish potato famine pathogen *Phytophthora infestans*. *Nature* 461:393–398.
32. Angot A, Vergunst A, Genin S, Peeters N (2007) Exploitation of eukaryotic ubiquitin signaling pathways by effectors translocated by bacterial type III and type IV secretion systems. *PLoS Pathog* 3:e3.
33. Van der Hoorn RA, Laurent F, Roth R, De Wit PJ (2000) Agroinfiltration is a versatile tool that facilitates comparative analyses of Avr9/Cf-9-induced and Avr4/Cf-4-induced necrosis. *Mol Plant Microbe Interact* 13:439–446.
34. Tian M, Huitema E, Da Cunha L, Torto-Alalibo T, Kamoun S (2004) A Kazal-like extracellular serine protease inhibitor from *Phytophthora infestans* targets the tomato pathogenesis-related protease P69B. *J Biol Chem* 279:26370–26377.
35. Grouffaud S, van West P, Avrova AO, Birch PRJ, Whisson SC (2008) *Plasmodium falciparum* and *Hyaloperonospora parasitica* effector translocation motifs are functional in *Phytophthora infestans*.. *Microbiology* 154:3743–3751.